AFOSR-TR· 90. 1204

②

SOUTHWEST RESEARCH INSTITUTE
Post Office Drawer 28510, 6220 Culebra Road
San Antonio, Texas 78228-0510

AD–A230 361

STUDY OF HIGH TEMPERATURE FAILURE MECHANISMS IN CERAMICS

By
Richard A. Page
James Lankford
Kwai S. Chan

**DTIC
ELECTE
JANO9 1991
S B D**

AFOSR ANNUAL REPORT

Approved for release; distribution unlimited.

November 1990

Approved:

Gerald R. Leverant, Director
Department of Materials and Mechanics

91 1 9 . 012

REPORT DOCUMENTATION PAGE

Public reporting burden for this collection of information is estimated to average 1 hour per response, including the time for reviewing instructions, searching existing data sources, gathering and maintaining the data needed, and completing and reviewing the collection of information. Send comments regarding this burden estimate or any other aspect of this collection of information, including suggestions for reducing this burden, to Washington Headquarters Services, Directorate for Information Operations and Reports, 1215 Jefferson Davis Highway, Suite 1204, Arlington, VA 22202-4302, and to the Office of Management and Budget, Paperwork Reduction Project (0704-0188), Washington, DC 20503

1. AGENCY USE ONLY (Leave blank)	2. REPORT DATE	3. REPORT TYPE AND DATES COVERED
	November 1990	Annual Report (Dec. '89 – Nov. '90)

4. TITLE AND SUBTITLE
High Temperature Failure Mechanisms in Ceramics

5. FUNDING NUMBERS
Contract F49620-88-C-0031

6. AUTHOR(S)
R. A. Page, J. Lankford, and K. S. Chan

7. PERFORMING ORGANIZATION NAME(S) AND ADDRESS(ES)
Southwest Research Institute
6220 Culebra Road
San Antonio, Texas 78228-0510

8. PERFORMING ORGANIZATION REPORT NUMBER
SwRI-2253/2

9. SPONSORING/MONITORING AGENCY NAME(S) AND ADDRESS(ES)
Dr. Liselotte J. Schioler   BΩ 410
Air Force Office of Scientific Research
Bolling Air Force Base
Washington, D. C. 20332

10. SPONSORING/MONITORING AGENCY REPORT NUMBER
2306 A2

11. SUPPLEMENTARY NOTES

12a. DISTRIBUTION/AVAILABILITY STATEMENT
Unlimited

12b. DISTRIBUTION CODE

13. ABSTRACT (Maximum 200 words)

This annual report documents the results of a basic research program aimed at (1) studying the high temperature failure mechanisms in ceramics, (2) establishing relationships between cavitation mechanisms and creep crack growth characteristics, and (3) developing a damage mechanism-based life prediction model. During the reporting period, the growth rate, near-tip creep responses, and damage processes of creep cracks in a pyroceram glass-ceramic were studied under tensile loading at elevated temperatures. The results of these studies indicated that creep crack growth in the pyroceram glass-ceramic occurred both in continuous and discontinuous manners, with the damage processes manifested as the nucleation, growth, and coalescence of inhomogeneously distributed cavities and microcracks. Sintering of cavities led to the existence of a growth threshold below which the creep crack would open, blunt, but not propagate. Measurements of the total accumulated creep strain near the crack-tip revealed that creep crack extension followed a critical strain criterion. Relationships between cavitation mechanisms and creep crack growth characteristics of the glass-ceramic are discussed.

14. SUBJECT TERMS
Ceramics, glass-ceramics, creep crack growth, cavitation mechanisms, creep crack growth threshold

15. NUMBER OF PAGES

16. PRICE CODE

17. SECURITY CLASSIFICATION OF REPORT	18. SECURITY CLASSIFICATION OF THIS PAGE	19. SECURITY CLASSIFICATION OF ABSTRACT	20. LIMITATION OF ABSTRACT
Unclassified	Unclassified	Unclassified	Unlimited

I. INTRODUCTION

A. Scope

Because of the attractive properties of ceramics at elevated temperatures, there is great interest in developing a new generation of aerospace propulsion systems capitalizing on advanced ceramics technology. These new propulsion systems would potentially offer higher operating temperatures and lower weights, thus providing dramatic increases over current engine designs in both efficiency and performance. While present engines utilize hot-stage components fabricated from nickel or cobalt-base superalloys, it is anticipated that evolving ceramic turbines will be based on silicon nitride and silicon carbide. In service, the ceramic components will experience tensile and/or cyclic loadings. Very little is known, however, about the behavior of these ceramics under tensile creep or cyclic creep conditions. An understanding of the basic failure mechanisms and an ability to predict lifetimes will be necessary before ceramics can be successfully utilized in engine applications.

B. Objectives and Approaches

The primary objectives of this basic research program are to characterize the creep damage accumulation processes in high temperature structural ceramics and to develop a predictive creep lifetime model based on the damage mechanism information. The approaches for achieving these goals are as follows:

1. Identify creep cavitation mechanisms in ceramics subject to tensile creep using scanning and transmission electron microscopies.

2. Utilize small-angle neutron scattering and other appropriate techniques to characterize cavity nucleation and growth rates under tensile creep conditions as functions of time, temperature, stress, strain rate, and microstructure.

3. Characterize creep crack growth and experimentally measure, using stereoimaging strain analysis, the crack-tip displacement field, strain distribution, and creep strain rates as functions of stress intensity, temperature, and microstructure.

4. Incorporate the cavitation model and measurements and the crack-tip micromechanical measurements into a fundamental creep crack growth model for ceramics.

II. STATUS OF THE RESEARCH EFFORT

Proposed research efforts for this program include studies of high temperature failure mechanisms, crack growth behavior, and crack-tip micromechanics of creep cracks in ceramics. As a continuation of the first year efforts [1], the research efforts in the last year were focused on establishing quantitative relationships between cavitation mechanisms, crack-tip micromechanics, and creep crack growth kinetics. For these studies, a magnesium-aluminosilicate glass-ceramic (Corning 9606 pyroceram) was employed as a model material representative of liquid-phase sintered ceramics. The microstructure of the glass-ceramic was typical of those commonly found in

many liquid-phase sintered ceramics, and it consisted of ≈ 0.5 μm diameter cordierite grains surrounded by an amorphous grain boundary phase which softens at $\approx 600°C$. Once the amorphous phase starts to soften, deformation of the glass-ceramic occurs by a combination of grain boundary sliding and cavitation.

During the last year, the creep crack growth characteristics of the glass ceramic were characterized as a function of temperature by testing inside a scanning electron microscope (SEM) equipped with a high-temperature loading stage. During the creep crack growth experiments, the near-tip region of the creep crack was photographed as a function of time of creep. Still photographs of the near-tip region from different times of creep were analyzed using the machine-vision-based stereoimaging technique [2], which was developed at SwRI, to obtain the near-tip displacement and the creep strain fields. Replication techniques were also used to characterize quantitatively the damage processes that accompanied creep crack growth. Relationships between the damage mechanisms and the crack growth processes were identified, including the origin of the growth threshold and the criterion for creep crack growth in the $K > K_{th}$ regime. In particular, the threshold for creep crack growth in the glass-ceramic was shown to arise from sintering of creep cavities at stress intensity, K, levels below the threshold, K_{th}. At $K > K_{th}$, creep crack growth was found to extend according to a critical creep strain criterion, which might in fact be an indication of a critical damage criterion for creep crack growth.

In addition to creep crack growth experiments involving pre-cracked specimens, creep experiments of smooth specimens were performed under compression, while those involving tensile loading are currently underway. These experiments were intended to provide information on cavitation kinetics; damage development in the creep specimens would be characterized using the small-angle neutron scattering (SANS) technique [3,4]. Efforts to develop a life prediction model based on the information on damage mechanisms during creep crack growth were initiated. Extension of the creep crack growth experiments to zirconia had been attempted as an effort to examine the generality of the creep damage processes in the pyroceram glass-ceramic. Creep testing of the zirconia was performed in the SEM loading stage at 800°C, but significant creep was not observed due to the relatively low test temperature. Since the maximum temperature capacity of the SEM stage is $\approx 800°C$, *in-situ* creep testing of zirconia or other structural ceramics at temperatures higher than 800°C would not be likely unless the high temperature capacity of the loading stage is increased. Future creep crack growth experiments of structural ceramics would thus be performed outside the SEM loading stage. Discussion of the more important results obtained in the last reporting period are presented in the next five sections.

A.   Characterization of the Creep Crack Growth Process

In-situ observations of creep crack growth experiments performed inside the SEM stage revealed that creep crack growth in the pyroceram glass-ceramic occurred either in a continuous or discontinuous manner [5]. During continuous growth, the main crack tip extended without any visible microcracking directly ahead of the crack tip. In contrast, discontinuous crack growth occurred with the formation of one or more microcrack(s) ahead of the crack tip. Further crack extension required the linkage of the microcrack(s) with the main crack; this process could take as much as 30 minutes or more. In some instances, the linkage of the microcrack and main crack was not complete, leaving ligaments which bridged the crack surfaces.

The creep crack growth rates were measured as a function of the stress intensity factor, K, at 700, 750, and 775°C. These results for the latter two temperatures are presented in Fig. 1, which shows that the crack growth rates can be correlated in terms of the K parameter. At both 750 and 775 C, the crack growth curve showed a threshold, K_{th}, below which no detectable crack growth occurred. The threshold was determined by unloading the propagating creep crack in small load increments until it was arrested. The K level was then increased until the crack resumed propagation. A duplicate specimen was used to verify the growth threshold by testing at $K \approx K_{th}$ under increasing K levels without prior unloading. The same K_{th} values were obtained in both cases, indicating the observed growth threshold is a material property of a large crack and not a load-history effect due to unloading.

B.   The Origin of the Creep Crack Growth Threshold

The observation of a threshold for creep crack growth in the glass-ceramic is consistent with previous findings on alumina and silicon carbide, which indicated the existence of a growth threshold for creep cracks that originated from pre-existing flaws (i.e., large cracks) in the ceramics. A growth threshold, however, was not observed in creep cracks that were initiated by creep damage. For life prediction, a growth threshold can significantly affect the predicted creep rupture life. Identifying the origin of the growth threshold for creep cracks in ceramics is therefore important. This was accomplished by performing the critical experiments which are discussed below.

The observed K_{th} value for the pyroceram glass-ceramic was ≈ 0.6 MPa$\sqrt{m}$ at 775°C. In order to investigate its origin, a fatigue-precracked specimen of the glass-ceramic was crept inside the SEM loading stage at 775°C under a stress intensity factor of 0.59 MPa$\sqrt{m}$. The near-tip region of the creep crack was photographed at 30 minute intervals. Photographs of the same region taken under identical K levels, but of different times of creep were analyzed for crack opening displacements and crack-tip strain distributions using the machine-vision-based stereoimaging technique. The surfaces of the creep crack were found to open, with the crack opening displacements increasing with increasing times of creep. Furthermore, the creep crack was found to propagate at $\approx 1 \times 10^{-6}$ m/hr. After 390 minutes of creep, the specimen was removed from the loading stage, and one of its surfaces was ion-milled for four hours. The surface of the specimen was replicated; the replicas were examined in a transmission electron microscope to evaluate the level of creep damage in the cracked specimen. The specimen was found to be heavily cavitated, but contained no well-defined microcracks. The formation of creep cavities ahead of the crack tip at K = 0.59 MPa $\sqrt{m}$ is illustrated in Fig. 2 (a). After damage characterization, the specimen was returned to the SEM loading stage for additional creep testing at 775°C for 8 hours at K = 0.59 MPa $\sqrt{m}$. The creep crack was observed to open, blunt, and extend during this period. The K level was then lowered to 0.5 MPa $\sqrt{m}$ and crept for 10 hours during which period the crack was observed to open, blunt, but not propagate. The result indicated the K level was below the growth threshold. The specimen was removed from the SEM stage, ion-milled, and replicated. Fig. 2 (b) shows the near-tip region of the creep crack, which indicates that all the previously observed near-tip cavities had disappeared. This observation indicated that the growth threshold of the glass-ceramic originated from sintering of creep cavities and removing of creep damage from the cracked specimen including the crack-tip region. This result is in agreement with a previous model [6] which predicted that sintering of cavities at the crack tip would lead to an abrupt drop in the creep crack growth rate and the formation of a threshold below which creep crack growth would not occur.
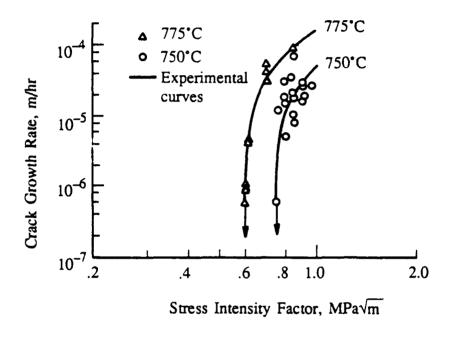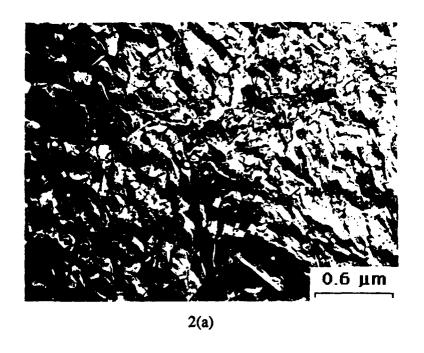
Figure 1.   Creep Crack Growth Curves for the Pyroceram Glass-Ceramic Showing the Existence of a Growth Threshold.
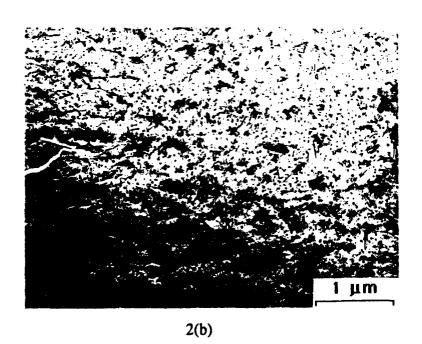
2(a)

2(b)

Figure 2. Comparison of the Near-Tip Cavitation Processes in the Pyroceram Glass-Ceramic at
K Levels At and Below the Growth Threshold: (a) Formation of Creep Cavities at K
$\geq K_{th}$; (b) Removal of Creep Cavities by Sintering at $K < K_{th}$.

5

In addition, the creep crack was also found to exhibit different near-tip strain distribution and crack surface opening behavior at K levels at and below the growth threshold, K_{th}. Comparison of the near-tip strain distributions for $K = 0.59$ MPa$\sqrt{m}$ and $K = 0.5$ MPa$\sqrt{m}$ is shown in Fig. 3. For $K = 0.59$ MPa $\sqrt{m}$, the region where the near-tip cavities were observed was represented by a line-contour, which was superimposed in the plot of the near-tip strain distribution in Fig. 3(a). Such a comparison revealed that regions of higher creep strain generally correspond to regions of high creep cavity density. Thus, the difference in the near-tip strain distribution observed at $K = K_{th}$ for a propagating crack and at K levels below K_{th} for a nonpropagating crack was due to the difference in the near-tip damage accumulation process. At $K = K_{th}$, cavities were nucleated near the crack tip, leading to creep crack growth. In contrast, cavities were not nucleated, but sintered at the crack tip at K levels less than K_{th}.

The rates of crack surface opening for the creep crack at $K = 0.5$ MPa $\sqrt{m}$ are compared with those for $K = 0.59$ MPa $\sqrt{m}$ in Fig. 4. The comparison revealed that the creep crack exhibited crack opening displacement rates at $K = 0.5$ MPa $\sqrt{m}$, but their magnitudes were lower than those observed at $K = 0.59$ MPa $\sqrt{m}$. The finite rate of crack opening displacement indicated that the crack tip continued to blunt by creep at K levels below the growth threshold, even though no cavities or crack extension were generated. These observations suggested that at least two different deformation mechanisms were operative at K levels at and above the growth threshold. One of these mechanisms, which is probably grain boundary sliding, led to cavitation, while the other, which is probably creep (diffusion or solution-reprecipitation), resulted in crack-tip blunting, but no cavitation. Based on the results shown in Figs. 2-4, it is clear that the growth threshold originates from a healing process which removes creep damage by the sintering of cavities. Physically, the growth threshold represents the stress intensity level at which cavity nucleation occurs near the crack tip and below which sintering of these cavities commences.

C.   Criterion For Creep Crack Growth

At $K > K_{th}$, creep crack growth occurred by accumulation of creep strain and cavitation damage near the crack tip. In order to develop a better understanding of this process, both the near-tip creep strain and cavitation damage were quantitatively characterized [5]. The near-tip cumulative creep strain measurement was obtained by the machine-vision-based stereoimaging technique. The experimental procedures for these measurements involved taking high-resolution micrographs of the crack tip region in a scanning electron microscope. The micrographs were taken both before and after creep crack growth into the region of interest. This pair of photographs was then analyzed to obtain the cumulative creep strain using the stereoimaging technique. Examples of these strain measurements for non-growing and growing creep cracks are shown in Fig. 5. The figure shows that the cumulative creep strain for the stationary crack after 230 minutes of creep was $\approx 0.8\%$. Creep strain accumulated to a higher value when the time of creep increased. After 375 minutes of creep, the crack started to propagate when the cumulative creep strain near the crack tip reached approximately 2%. These results indicated that creep crack growth in the model ceramic obeyed a critical cumulative strain criterion. The critical cumulative creep strain was measured for various K levels and times of creep which are shown in Fig. 6. The results indicate that the critical value of the cumulative creep strain for creep crack growth is approximately 2%, and it is independent of K level and time of creep.
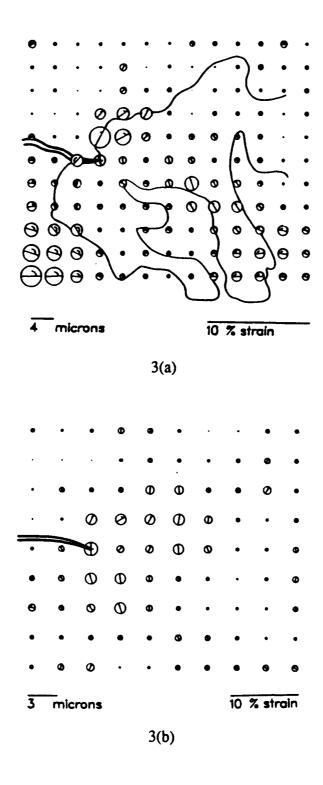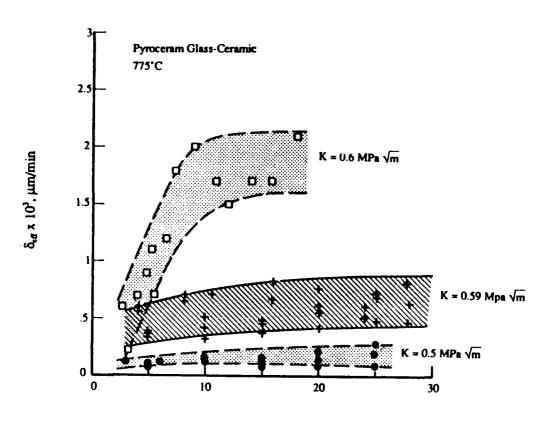
3(a)

3(b)

Figure 3. Comparison of the Near-Tip Creep Strain Distributions at Two K Levels: (a) K = K_{th}; and (b) K < K_{th}. The line contour in (a) represents the region within which creep cavities are located.

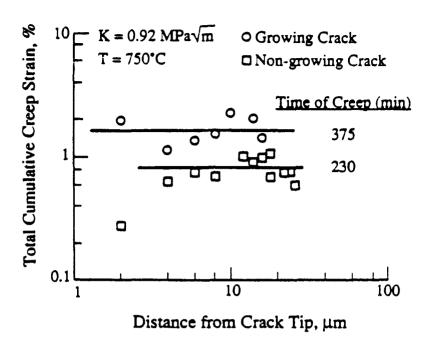Figure 4. Comparison of the Crack Surface Opening Displacement Rates at K Levels At and Below the Growth Threshold.

Figure 5.   Comparison of Total Cumulative Creep Strains for a Creep Crack in the Nonpropagating and Propagating Conditions.
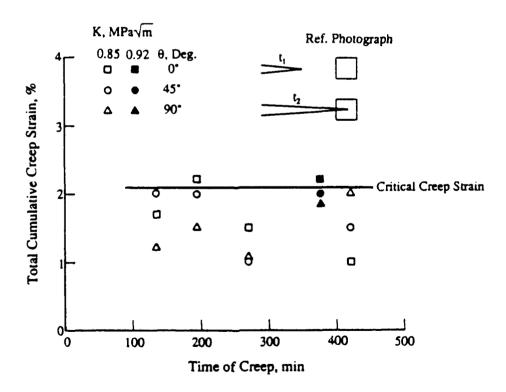

Figure 6.   Critical Values of the Total Cumulative Creep Strain for Various Times of Creep.

D.   Characterization of Creep Damage

The damage processes which occurred during creep crack growth in the pyroceram glass-ceramic were identified by direct observations of the crack extension sequence *in-situ* via the SEM and by examining replicas of the surfaces of the specimens via scanning and transmission electron microscopies. As indicated earlier, *in-situ* observation revealed that creep crack growth occurred by either a continuous or discontinuous process. Consistent with this observation, the replicating technique revealed the presence of two different cavitation defects in the glass-ceramic. These two types of creep-induced damage are shown in Fig. 7, and they include (1) pockets of heavily cavitated regions of creep cavities, and (2) microcracks that are comprised of a row of cavities aligned in a linear fashion. In both cases, the creep cavities located within the pockets or the microcracks are generally of approximately equal size, spacing, and shape. An incipient microcrack formed by this process is shown in Fig. 8. Based on the similarity in cavity size, shape, and spacing, it appears that the creep cavitation process could have occurred through two possible mechanisms. The first possible mechanism was that all the creep cavities were nucleated at the same time, and they exhibited equivalent growth rates until coalescence. The second possible mechanism, which is considered more plausible, is a cavitation process which involves the nucleation of cavities that could not grow beyond a critical size. Under this circumstance, cavitation is dominated by continuous nucleation of cavities until the cavities are sufficiently close for coalescence to take place. The nucleation of cavities is in turn controlled by stochastic grain boundary sliding and the availability of potential nucleation sites [7], both are governed by the microstructure of the grain boundaries. Such a process of nucleation dominated cavitation with cavities which would not grow beyond a critical size has been observed in Lucalox and AD99 alumina [3,4], the latter is a liquid-phase, sintered ceramic which contains an amorphous phase along grain boundaries, as in the pyroceram glass-ceramic.

Both the microcracks and heavily cavitated regions were inhomogeneously distributed throughout the microstructure. It was quite common for one region to be heavily cavitated, while the contiguous regions were cavity-free, as shown in Figs. 7 and 8. In order to better understand the damage process, qualitative measurement techniques were used to characterize the distribution of microcracks and the heavily cavitated regions. For illustration, Fig. 9 shows the distribution of microcracks observed ahead of the tip of the creep crack in the pyroceram glass-ceramic. The microcrack density was measured as a function of distance ahead of the crack tip, and the results are presented in Fig. 10. Additionally, the area fraction of heavily cavitated regions is shown in Fig. 11. The results indicated that both the microcrack density and the area fraction of heavily cavitated regions increased with decreasing distance from the crack tip. Based on these results, it can be suggested that the critical cumulative strain criterion observed in Figs. 5 and 6 might in fact be an indication that creep crack growth in the ceramic is dictated by attaining a critical level of creep damage.

E.   Life Prediction Modeling

The development of a life prediction model based on the cavitation damage mechanisms is in the initial stage. Conceptually, the life prediction model would be based on the relevant experimental observations of the cavitation process [5,8], which are summarized in the schematic shown in Fig. 12. Experimental observation revealed that creep cavitation damage was related to the creep rate. The proposed model would therefore be formulated by considering the creep rates as functions of time, K levels, distance ahead of the crack tip, and the damage process. Observa-
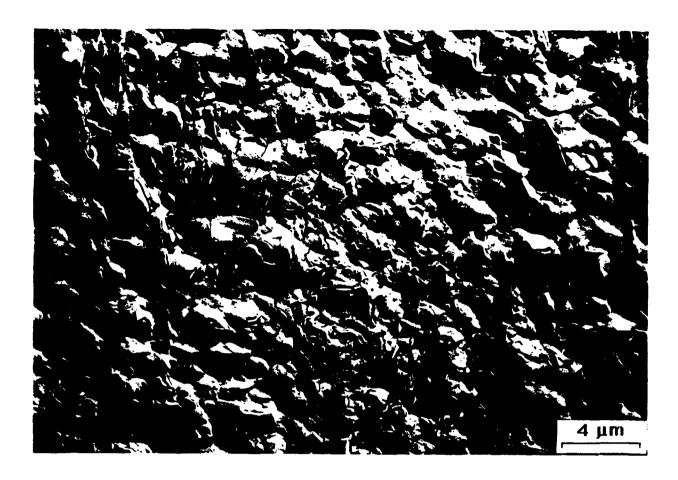
Figure 7. TEM Replica Showing a Microcrack and a Pocket of Creep Cavities Surrounded by Relatively Uncavitated Regions.
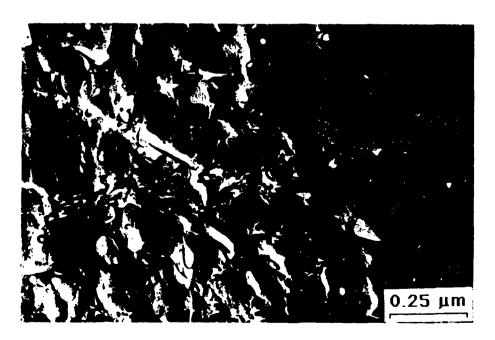

Figure 8. An Incipient Microcrack Formed by Creep Cavities of Approximately Equal Size, Shape, and Spacing Aligned in a Linear Fashion.
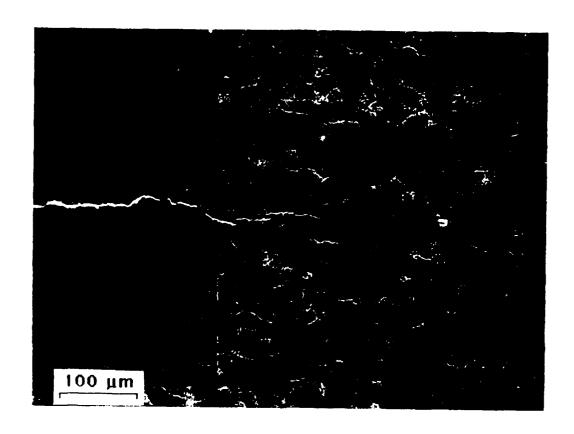
11

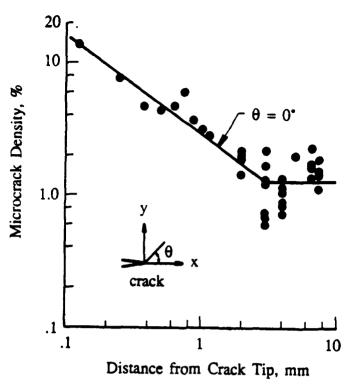Figure 9. Microcracks Observed Near the Tip of the Main Crack in Pyroceram.

Figure 10. Microcrack Density as a Function of Distance from the Tip of the Main Crack Tested at 750°C and K = 0.92 MPa √m.
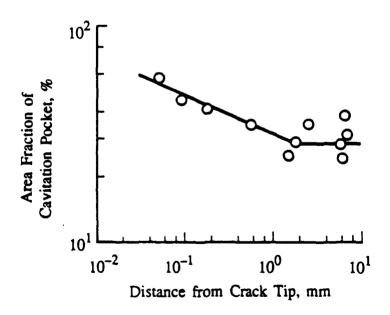

Figure 11. Area Fraction of Cavitated Region as a Function of Distance Ahead of the Main Crack Tested at 750°C and K = 0.92 MPa √m.
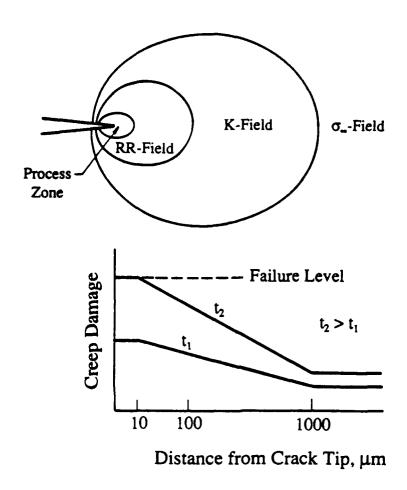
Figure 12. Schematic of the Creep Crack Growth and Damage Accumulation Process Utilized in the Proposed Life Prediction Model.

tions based on the crack-tip micromechanic experiments indicated that the creep cavitation and crack growth process in the pyroceram glass-ceramic were the same as those described in Fig. 12. In this process, creep damage accumulates within a "process zone" located ahead of the tip of the creep crack. The "process zone" is embedded within the Ridel-Rice (RR) field [9], which is, in turn, surrounded by the K-field and the field due to the remote stress, σ_∞. Creep damage within the "process zone" increases with increasing time of creep, and the creep crack extends when the creep strain or the amount of creep damage within the process zone reaches a critical value. Healing of creep damage by sintering of creep cavities will be incorporated into the model describing the damage evolution in the process zone. The sintering term is expected to result in a growth threshold for creep cracks originated from large pre-existing flaws.

The proposed modeling approach is consistent with all the experimental observations [5,8] with one exception, which is the size of the "process zone." The near-tip creep strain measurements indicated that the process zone, which appeared as a localized shear channel in the creep strain distribution, was on the order of 50 μm. On the other hand, damage characterization based on the replication techniques revealed extensive creep damage in the form of both microcracks and pockets of heavily cavitated regions throughout the specimens, indicating that the "process zone" might be the width of the remaining ligament. Furthermore, model development requires resolving the apparent discrepancy of the "process zone" size. A critical experiment aimed at identifying the damage processes that occurs within the shear channel is currently underway to generate information which would help resolve the issue of the critical "process zone" size.

F. References

1. R. A. Page, J. Lankford, and K. S. Chan, "Study of High Temperature Failure Mechanisms in Ceramics," AFOSR Annual Report, Contract F49620-88-C-0081, 1989.

2. D. L. Davidson, K. S. Chan, and R. A. Page, in Micromechanics: Experimental Techniques, edited by W. N. Sharpe, Jr., AMD. Vol. 102, 1989, pp. 73-87.

3. R. A. Page, J. Lankford, and S. Spooner, *Acta Met.*, Vol. 32, 1984, p. 1275.

4. R. A. Page, J. Lankford, K. S. Chan, K. Hardman-Rhyne, and S. Spooner, *J. Am. Ceram. Soc.*, Vol. 70, 1987, p. 137.

5. K. S. Chan and R. A. Page, "Creep Crack Growth by Damage Accumulation in a Glass-Ceramic," *J. of the Am. Cer. Soc.*, 1990 (submitted).

6. M. D. Thoules and A. G. Evans, *Scripta Met.*, Vol. 18, 1984, pp. 1175-1180.

7. K. S. Chan and R. A. Page, "Transient Cavity Growth in Ceramics Under Compression," *J. Mat. Science*, 1990 (submitted).

8. R. A. Page, K. S. Chan, D. L. Davidson, and J. Lankford, "The micromechanics of Creep Crack Growth," *J. Am. Cer. Soc.*, Vol. 73, No. 10, 1990, pp. 2977-2986.

9. H. Riedel and J. R. Rice, *J. Mech. Phys. Solids*, Vol. 29, 1981, pp. 35-49.

III. ACCOMPLISHMENTS

The significant accomplishments achieved in this program during the last year are as follows:

1. The mechanisms of creep crack growth were identified for a model ceramic. Correlations between creep crack growth rates and the stress intensity factor were established.

2. Sintering of cavities was identified as the mechanism leading to the growth threshold below which a creep crack does not propagate.

3. A critical creep strain criterion for creep crack growth in a glass-ceramic was identified.

4. The creep damage processes associated with creep crack growth in the model ceramic were identified. Relationships between cavitation mechanisms and crack growth kinetics were partially established.

IV. FUTURE WORK

Although some basic understanding has been developed, there are several aspects of the creep cavitation and crack growth processes in ceramics that are still not fully understood. Some examples of the critical areas are the lack of understanding of the damage mechanisms that lead to the formation of the localized shear zone which was previously observed ahead of the creep crack, the critical damage criterion for crack extension, the crack size dependence of the growth threshold during crack propagation, and the relationships between cavitation kinetics and crack growth rates. These critical issues will be addressed by future work in this program. This work includes the following:

1. Continue crack-tip micromechanics and crack growth characteristics studies of creep cracks to investigate the failure processes for creep cavitation in ceramics.

2. Characterize cavitation kinetics using the small-angle neutron scattering technique to study damage evolution as a function of temperature, stress, and microstructural effects.

3. Develop damage accumulation and creep crack growth models for lifetime prediction.

V. PUBLICATIONS (AFOSR SPONSORSHIP)

1. "Automated High-Resolution Displacement Measurements for Deformation and Fracture Research," by D. L. Davidson, K. S. Chan, and R. A. Page, in Micromechanics: Experimental Techniques, ASME, edited by W. N. Sharpe, Jr., AMD-vol. 102, 1989, pp. 73-87.

2. "The Micromechanics of Creep Crack Growth in a Glass-Ceramic," by R. A. Page, K. S. Chan, D. L. Davidson, and J. Lankford, *Journal of the American Ceramic Society*, Vol. 73, No. 10, 1990, pp. 2977-2986.

3. "Near-tip Behavior of Deflected Creep Cracks," by K. S. Chan, R. A. Page, and D. L. Davidson, *International Journal of Fracture*, 1990 (in press).

4. "Creep Crack Growth by Damage Accumulation in a Glass-Ceramic," by K. S. Chan and R. A. Page, *Journal of the American Ceramic Society*, 1990 (submitted).

5. "The Origin of the Creep Crack Growth Threshold in a Glass-Ceramic," by K. S. Chan and R. A. Page, *Journal of the American Ceramic Society*, 1990 (in preparation).

VI. INTERACTIONS

"Creep Crack Growth in a Glass-Ceramic Material," by R. A. Page and J. Lankford, 91st Annual Meeting of the American Ceramic Society, Indianapolis, IN, April 1989.

VII. PROGRAM PERSONNEL

Name	Title	
Dr. Richard A. Page	Staff Scientist and Section Manager	} Co-Principal
Dr. James Lankford	Institute Scientist	} Investigators
Dr. Kwai S. Chan	Principal Engineer	
Mr. Harold G. Saldana	Supervisor	
Mr. John B. Campbell	Staff Technician	
Mr. James S. Spencer	Staff Technician	

APPENDIX

CREEP CRACK GROWTH BY DAMAGE
ACCUMULATION IN A GLASS-CERAMIC

K. S. Chan   and R. A. Page,

Southwest Research Institute,

San Antonio, TX, 78228-0510

The growth rate, near-tip creep response, and damage processes of creep cracks in pyroceram glass-ceramic were studied at elevated temperatures. The rates of crack extension were characterized as a function of the applied stress intensity factor. The damage processes which occurred near the crack tip and led to creep crack extension were identified using a replica technique and by direct observations in a scanning electron microscope equipped with a high temperature loading stage. The accumulated creep strains near the crack tip were measured via the stereoimaging technique. The results indicate that creep crack growth in a pyroceram glass-ceramic occurs both in continuous and discontinuous manners, with the damage processes manifested as the nucleation, growth and coalescence of inhomogeneously distributed cavities and microcracks. Measurements of the total accumulated creep strain near the crack-tip suggest that crack extension follows a critical strain criterion. Both the microcrack density and the total accumulated creep strain show similar dependence with distance from the crack tip. These observations suggest that damage accumulation and crack extension in the glass-ceramic are controlled by the near-tip creep rates.

INTRODUCTION

Subcritical crack growth has been observed in a number of ceramics under elevated temperature loading [1-13]. Such subcritical or creep crack growth is generally characterized by intergranular fracture paths, and occurs by the nucleation, growth, and coalescence of grain boundary cavities and/or microcracks ahead of the crack tip [8-13]. Typically, creep crack growth in ceramics occurs at stress intensities, K, between a threshold, K_{th}, and a critical value, K_C, which represents the onset of unstable fracture [12,13]. Below the threshold, creep cracks blunt, exhibit crack opening displacement, but no longer propagate. Furthermore, a near-tip strain distribution different than that of propagating creep cracks was observed for cracks below the threshold [14]. Above the threshold, creep crack growth is characterized by a power-law relation between the crack velocity and the stress intensity factor [12,13].

For ceramics with pre-existing flaws, creep cavities might be localized and occur predominantly near the tip of the creep crack, forming a creep damage or fracture process zone [8-13]. This damage zone consists of individual and/or coalesced cavities. The linkage of the creep cavities with the tip of the main crack constitutes a crack extension event and occurs in an incremental and discontinuous manner. The incremental nature of the crack extension process suggests that a critical amount of creep strain and/or damage must be accumulated within the damage zone prior to crack extension. The rate of creep crack extension thus depends on the rate, and the nature, of the damage accumulation process within the process zone, both of which are expected to be influenced by the local stresses and strain rates near the tip of the creep crack, as well as by the microstructure of the ceramics [12], e.g., the presence of a vitreous grain boundary phase. In particular, creep cracks in vitreous-bonded materials tend to propagate along the grain boundary vitreous phase, occasionally

leaving intact ligaments of the vitreous phase behind the crack tip [11]. These amorphous ligaments are subjected to shear deformation and offer resistance to further creep crack propagation by exerting tractions on the crack surface, thereby reducing the local driving force for crack extension [12,15].

The development of creep damage is an essential process for extension of a creep crack. However, little work has been done to characterize the creep damage process ahead of a creep crack, and its impact on, or relationship to, creep crack growth. The incorporation of creep damage into a creep crack growth model has been attempted by Thouless and Evans [15]. A key feature of their model is that the creep crack growth rate depends sensitively on the ratio of cavity spacing to grain facet length, which represents the degree of local creep damage within the process zone. Characterizing the development of creep damage during creep crack growth is therefore important for improving the current understanding of the creep crack growth process in ceramics.

The objective of this paper is to characterize the damage process associated with creep crack growth in a pyroceram glass-ceramic. This work is a follow-on of a previous paper [14] which examines the micromechanics of creep crack growth in the pyroceram glass-ceramic. While the previous paper is concerned with the near-tip creep deformation, the present paper is focused on the relationship between the near-tip damage process and the resulting crack growth behavior. In particular, the creep crack growth rate will be measured as a function of the stress intensity factor, K. A machine-vision-based stereoimaging technique will be used to measure the creep strains accumulated within the damage process zone prior to crack extension. The type and extent of creep damage in the glass-ceramic will be identified and measured as a function of distance from the crack tip. These results will be utilized with near-tip strain measurements to examine whether a critical amount of creep damage or accumulated strain within the process zone is required for creep crack growth and to identify the relationship between creep damage and the crack growth curve.

EXPERIMENTAL PROCEDURES

Material

A magnesium-aluminosilicate glass-ceramic (Corning 9606), which consisted of 0.5 μm diameter cordierite grains surrounded by a thin continuous amorphous phase, was utilized for this study. Previous studies have indicated that the grain boundary vitreous phase of this glass-ceramic begins to soften at around 600°C [16,17]. Once the amorphous phase is softened, deformation occurs by a combination of grain boundary sliding and cavitation. This material is thus believed to be representative of the many liquid-phase-sintered ceramics. The creep exponent, n, of the cordierite glass-ceramic was ≈ 2[18], which was somewhat higher than the n-value of unity observed in the Corning 9608 lithium-aluminosilicate (LAS) glass-ceramics [19,20], but was consistent with n = 1.5 - 2.2 reported for other LAS glass-ceramics [21].

Crack Growth Rate Measurements

Creep crack growth in the pyroceram glass-ceramic was studied in the 700-775°C range using single-edge-notched specimens. The dimensions of the test specimens and the experimental procedures were identical to those reported earlier [14]. In particular, the specimens were pre-cracked by cyclic fatigue under compressive loads at room temperature. After cyclic fatigue pre-cracking, the specimens were coated with gold to provide a conductive surface and tested under a constant tensile load in a scanning electron microscope equipped with a high temperature loading stage [22]. The region in the vicinity of the crack tip was monitored and photographed in approximately 15-30 minute intervals using 1000-2000X magnifications. The amount of crack extension within a given time interval was obtained by measuring the length of the crack from the SEM photographs

taken before and after that time period. The crack velocity was computed by dividing the amount of crack extension by the time interval, and the stress intensity factor was computed using the formula due to Gray [23].

Near-Tip Cumulative Strain Measurements

The total creep strain accumulated in the region located near the tip of a crack prior to crack growth into that region was measured using a machine-vision-based stereoimaging technique [24]. The procedure for performing such strain measurements is shown schematically in Fig. 1. Prior to creep testing, the region located 100 μm directly ahead of the crack tip was photographed extensively as a reference area using the SEM. The creep crack growth experiment was then performed, and the referenced area was again photographed after the creep crack had extended into that region. The accumulated creep strain was then determined by analyzing photographs of the region before and after crack advance using the machine-vision-based stereoimaging technique described in [24]. Specifically, the stereoimaging technique measured the relative in-plane displacements of an array of material points in the region of interest. These displacements were used to obtain the displacement gradients, which were in turn used to compute the different in-plane strain components. A more detailed description of the strain measurement technique can be found in [25]. Since it was not known where the creep crack would advance, an extensive region ahead of the crack tip was mapped in order to obtain the accumulated strain measurements.

Characterization of Creep Damage

After the creep crack growth experiments, the test specimen was ion-milled for four hours to remove the conductive coating and any other surface contaminants. The specimen surface was then

replicated using acetobutyrate and cellulose acetate replicating tapes. The former was coated with aluminum and examined in the SEM, while the latter was coated with carbon, shadowed, dissolved, and examined via the TEM. The SEM and TEM micrographs were then used to characterize the distribution, size, and density of microcracks and cavities, using quantitative ceramographic techniques.

To describe the extent of microcracking, the crack density parameter proposed by Budiansky and O'Connell was adopted [26]. This particular crack density parameter, ε, is defined as [26]

$$\varepsilon = \frac{2N}{\pi} \langle \frac{A^2}{P} \rangle \qquad (1)$$

where N is the number of microcracks per unit volume, A is the area, and P is the perimeter of a microcrack. For n_i circular microcracks of length $2a_i$ in a local volume, V_l, the crack density parameter, ε, is

$$\varepsilon = \frac{n_i \langle a_i^3 \rangle}{V_l} \qquad (2)$$

which indicates that ε differs from the local volume fraction of microcracks in the sampling volume by a factor of $4\pi/3$. For the measurement techniques utilized in this study, it is more convenient to use a crack density parameter which is defined in terms of the area fraction of microcracks in a local sampling area. Motivated by Eq. (2), a crack density parameter, ψ, defined as

$$\Psi = \frac{n_i \pi (a_i^2)}{A_l} \qquad (3)$$

which is the fraction of "cracked area" in a local sampling area, A_1, is used to represent the local microcrack density. The repeated indices in Eq. (3) means summation. A geometric representation of the crack density parameter, ψ, is shown in Fig. 2. According to quantitative metallography [27], the area fraction and volume fraction of a "second phase" are equal, the crack density parameters of ε and ψ would be similar, but differ by a constant of $4\pi/3$. For the crack density measurements shown in this paper, a sampling square of 0.254 mm was used.

RESULTS

Crack Growth Behavior

The amount of crack extension in the pyroceram glass-ceramic tested at 750°C and a stress intensity factor of 0.85 MPa(m)$^{0.5}$ is presented in Fig. 3 as a function of time of creep. Similar results for creep crack growth at 700 and 750°C have been shown earlier in [14]. Previous results indicated that creep crack growth in the pyroceram occurred in a continuous manner at 775°C, but a discontinuous manner at 700°C. These two types of growth behavior were observed in-situ in the SEM, and are illustrated schematically in Fig. 4. As depicted in Fig. 4(a), continuous creep crack growth in the glass-ceramic occurred by direct extension of the main crack, without any visible microcracking directly ahead of the crack tip when viewed at 1000-2000X magnification. In contrast, discontinuous crack growth occurred with the formation of a microcrack ahead of the crack tip. Further crack extension required the linkage of the microcrack with the main crack, which was a process that could take as much as 30 minutes or more. In some instances, the linkage of the microcrack and main crack was not complete, leaving ligaments which bridged the crack surfaces. The crack extension curve in Fig. 3 shows periods of zero crack extension even though the crack length generally increased with time. The present results at 750°C confirmed the previous observation that creep crack growth could occur in either a continuous or discontinuous manner.

Fig. 5 summarizes the crack growth data as a function of the stress intensity factor, K, for 700, 750, and 775°C. The experimental curves were drawn through the data of 750 and 775°C. At both temperatures, the crack growth curve showed a threshold, K_{th}, below which no detectable crack growth occurred. The threshold was determined by unloading the propagating crack in small load increments until it was arrested. The K level was then increased until the crack resumed propagation.

A duplicate specimen was used to verify the growth threshold for 775°C by testing at $K = K_{th}$ under increasing K levels without prior unloading. The same K_{th} values were obtained in both cases, indicating the observed growth threshold is a material property of a large crack and not a load-history effect due to unloading. All of the test data at 700°C appeared to lie on the threshold portion of the crack growth curve. In this case, load shedding was not used. The present results are thus consistent with previous work on alumina [10] and silicon carbide [5], which indicated the existence of a growth threshold for creep cracks that originated from pre-existing flaws in the ceramics. A growth threshold, however, was not observed in creep cracks that were initiated by creep damage [11].

Accumulated Creep Strain

The total cumulative creep strains in the near-tip region of the creep crack were analyzed for various times of creep and crack propagation conditions. Fig. 6 shows a typical distribution of the total cumulative creep strain as a function of distance from the crack tip for a creep crack growing in a continuous manner 135 minutes after the onset of creep crack growth at $K = 0.85$ MPa(m)$^{0.5}$. The cumulative strain distribution is similar to the incremental creep strain distributions exhibited by creep cracks after long creep times that were reported earlier in [14]. In particular, the total cumulative creep strains are approximately constant near the crack tip, and they do not appear to fit the Riedel-Rice strain distribution.

The total cumulative strain distribution for a creep crack which grew in a discontinuous manner is shown in Fig. 7. At 230 minutes after the onset of creep crack growth, the crack was in a stationary position and the total cumulative creep strain ahead of the crack tip was approximately 0.8%. The crack remained stationary while creep strain accumulated within the near-tip region. After an additional 145 minutes of creep, the crack resumed propagation when the total cumulative

After an additional 145 minutes of creep, the crack resumed propagation when the total cumulative creep strain in the crack-tip region reached ≈ 2%. This result suggests that a critical value of 2% creep strain was required for fracture of the near-tip process zone. This critical value of total creep strain accumulated within the crack tip process zone prior to incremental crack extension was measured for various times of creep. These results, shown in Fig. 8, indicate that the critical value of the cumulative creep strain required for fracture of the crack-tip process zone is approximately 2%; this value does not appear to vary with the time of creep and, by implication, the amount of crack extension.

Microcrack Density

The development of creep damage ahead of a creep crack in the pyroceram ceramic was studied after creep crack growth at 750°C under a K level of 0.95 MPa(m)$^{0.5}$. Surface replicas revealed the presence of microcracks on the test specimen. The microcracks were concentrated near the tip of the main crack, as illustrated in Fig. 9. The microcracks, however, were not limited to the crack-tip region, but were distributed throughout the uncracked ligament. The distribution of the microcracks was studied by replicating and photographing across the width of the specimens at 200X magnification. A montage of the specimen was constructed from the SEM photographs showing the microcracks. Fig. 10 shows traces of microcracks located in a region which is within 2 mm of the tip of the creep crack. As shown in Fig. 10, the microcracks are on the order of 10-40 μm. The smaller microcracks show no preferred orientation with respect to the loading axis. The larger microcracks have a tendency to align normal to the loading axis and they are generally formed by the linkage of smaller microcracks.

The maximum microcrack size is shown as a function of distance from the crack tip in Fig. 11, while the number of microcracks per unit area is shown in Fig. 12. In general, both the number and the size of the microcracks decrease with increasing distance form the crack tip. At distances greater than 1 mm from the crack tip, the number and the size of the microcracks appear not to vary with distance. Fig. 13 shows the value of the microcrack density parameter, ψ, as a function distance, r, ahead of the crack tip. For distances in the range of 0.1 mm to 2 mm from the crack tip, the microcrack density, as measured by ψ, decreases with increasing distance from the crack tip, but remains relatively constant at r>2 mm. There is also more local variation in the microcrack density parameter at r>2 mm.

Grain Boundary Cavities

TEM replicas revealed that many grain boundaries in the pyroceram test specimen were cavitated. During creep crack growth, grain boundary cavities were nucleated, subsequently grew, and coalesced to form microcracks, as shown in Fig. 14. Detailed examination of these microcracks at high magnification revealed that they were formed by the coalescence of rows of equally spaced and sized grain boundary cavities; such an example is shown in Fig. 15. Microcracks, which were initiated at triple-points of grain boundaries and grew into grain facet cracks, were seldom observed. The creep cavities were inhomogeneously distributed throughout the specimen. Some regions of the specimen showed a relatively large concentration of cavities, while the neighboring areas were denuded of cavities. In most instances, the heavily cavitated areas appeared as pockets of cavities surrounded by uncavitated grain boundaries, as illustrated in Fig. 16. These regions of high cavity density had an average diameter of approximately 40 μm. In addition to these volumetric pockets of high cavity density, more or less linear arrays of contiguous, highly cavitated grain boundaries were also observed. The linear arrays of cavitated boundaries appeared to be an early stage of the

microcrack formation. The three dimensional pockets of high cavity density, on the other hand, did not generally appear to be involved in the formation of microcracks. In fact, it was not uncommon to have one or both of the tips of the microcracks end at these pockets of heavily cavitated areas, suggesting that the cavity pockets might have stopped propagation of the microcracks. Fig. 17 gives an example of a microcrack terminating at two pockets of cavities.

DISCUSSIONS

The present results indicate that two damage processes are associated with creep crack growth in the pyroceram glass-ceramic; they include (1) the nucleation, growth, and coalescence of grain boundary cavities which leads to the formation of microcracks, and (2) the propagation and linkage of microcracks with the main crack. These two damage processes are interconnected, with the former preceding and leading naturally to the latter. The observation of pockets of heavily cavitated regions surrounded by uncavitated regions suggests that there are preferred grain boundaries for cavity nucleation. Microstructural reasons for the presence of soft or easily cavitated regions encompassing hundreds or thousands of grains were not readily apparent. However, one could postulate that minor changes in the composition of the grain boundary glassy phase could affect the viscosity of the grain boundary phase and thus its resistance to sliding and cavitation. If this is indeed the reason for the inhomogeneous damage process, similar behavior could be expected in other ceramics containing amorphous grain boundary phases. The approximately equal size of the multiple cavities on a two-grain junction indicate that the cavities might be nucleated at the same time, possibly by the sliding of grain boundaries containing ledges. The coalescence of these cavities to form a facet-sized microcrack may occur either by the growth of the nucleated cavities or through the continued nucleation of cavities at ligaments located between the cavities.

The occurrence of both continuous and discontinuous crack growth in the pyroceram glass-ceramic appeared to be the direct consequence of the nonuniform distribution of cavities and microcracks ahead of the crack tip. Crack propagation through such a nonuniform damage field would be expected to occur in a more or less continuous manner through regions of heavy damage with periodic arrest periods when the crack tip encountered regions of low damage. A change of

the crack growth behavior from a continuous to a discontinuous mode or vice versa is therefore expected as the creep crack propagates through a nonuniform distribution of cavitated and uncavitated regions, as was observed experimentally.

The creep damaged area observed in the glass-ceramic was large, extending from the tip of the main crack to the opposite edge of the specimen. The large damage zone was characteristic of a crack subjected to a relatively high stress intensity factor over a relatively long period of time of creep. A previous study [14] has shown that the near-tip strain and crack opening behavior in the pyroceram glass-ceramic were those of the Riedel-Rice type [28] when the time of creep was short and the amount of crack extension was small. Furthermore, the crack opening displacement attained the steady-state condition after only 110 minutes of creep at a K level of 0.80 MPa(m)$^{0.5}$ and at 700°C. Since the creep damage characterization presented in this paper was performed for a creep crack that had been growing at K = 0.95 MPa(m)$^{0.5}$ and 750°C for more than 300 minutes, the large creep damage zone was probably the consequence of gross creep in the specimen. For small scale creep, the size, r_c, of the creep zone ahead of a creep crack is described by [28]

$$r_c \propto K^2 t^{2/(n-1)} \tag{4}$$

and the accumulated effective creep strain, $\bar{\epsilon}$, is

$$\bar{\epsilon} \propto K^{2n/(n+1)} t^{1/(n+1)} \tag{5}$$

$$\text{with} \quad \bar{\epsilon} = (2/3 \epsilon_{ij} \epsilon_{ij})^{1/2} \tag{6}$$

where n is the creep exponent, ε_{ij} is the strain tensor, and t is the time of creep. Since the creep exponent for the pyroceram ranges from 1.5 to 2.0 [18,21], both the creep zone and its rate of growth increase with time at a constant K level. Fig. 14 shows that the slope for the crack density parameter, ψ, versus distance, r, plot is ≈ 0.75, which is approximately the same as that for the radial dependence of creep strain in the Riedel-Rice field and those observed in the pyroceram for large r [14]. The similarity in the radial dependence suggests that the crack density might be proportional to the effective creep strain accumulated within the creep zone, i.e.,

$$\psi \propto \bar{\varepsilon} \tag{7}$$

which may be combined with Eqs. (4) and (5) to give

$$\psi \propto K^{2n/(n+1)}t^{1/(n+1)} \tag{8}$$

and

$$r_d \propto K^2 t^{2/(n-1)} \tag{9}$$

as the extent of the damage zone, r_d. The lack of a contained near-tip damage zone in the pyroceram glass-ceramic may then be directly attributed to two factors: (1) the relatively low n value ($1 \leq n \leq 2$) of the pyroceram, which causes both the damage zone size and its rate of growth to increase with time, and (2) a relatively large time of creep.

The observation of a critical accumulated effective creep strain for incremental crack extension lends support to the use of such an assumption in many creep crack growth models [29,30]. However, the relation between the crack density parameter, ψ, and the accumulated effective creep strain (Eq. 7) implies that the observed critical creep strain criterion may in reality be a manifestation of a critical crack density or creep damage criterion, i.e., crack extension occurs when the microcrack density or creep damage in the process zone attains a critical value. In fact, a critical crack density or creep damage criterion might be more consistent with experimental observations over the whole range of the crack growth curve, including the threshold region, than does a critical accumulated effective creep strain. In particular, previous observations both for the pyroceram glass-ceramics [14] and for other ceramics [5,10] indicate that crack-tip blunting accompanied the creep crack growth threshold. Since crack-tip blunting necessarily accumulates creep strain near the crack tip, a critical accumulated creep strain criterion would lead to crack growth and is, therefore, inconsistent with the observation of a growth threshold. On the other hand, crack-tip blunting at the growth threshold is acceptable in a critical crack density or creep damage criterion if crack-tip blunting occurs without causing damage accumulation near the crack tip. Indirect evidence of a change in the damage accumulation processes at K levels below and above the growth threshold is shown in Fig. 18. At $K>K_{*}$, creep crack growth in the pyroceram propagated along a localized shear channel of creep strain within which creep damage appeared to accumulate. Such a shear channel of creep strain is absent in creep cracks below the growth threshold, as shown in Fig. 18. The implication is that the formation of a localized channel of shear strain is important in the damage accumulation process, and the lack of a shear channel leads to the growth threshold. Since the first step in the process is the nucleation of grain boundary cavities, the growth threshold and the shear channel in the pyroceram might be related to cavity nucleation as suggested by Thouless and Evans [31].

16

Further studies of the damage accumulated around creep cracks loaded below their threshold are required to determine the origin of the shear channel and if crack growth is indeed a critical damage controlled process.

Another question concerning the creep crack growth curves shown in Fig. 5 is whether or not the stress intensity factor, K, is the relevant correlating parameter. Based on the analysis of Riedel and Rice, one would think the stress intensity factor would be applicable only for small creep conditions. On the other hand, Fig. 5 indicates that K appears to correlate the creep crack growth rates rather well for the pyroceram, even though gross creep and damage occurred at the higher K levels. Previously, Blumenthal and Evans [10] showed that K is the relevant parameter for correlating the creep crack growth data of alumina for which the creep exponent, n, has a value close to unity. The present results are consistent with those of Blumenthal and Evans [10]. One possible explanation of the applicability of K to the large creep conditions might be the relatively low n values (n = 1.5-2) for the pyroceram, which is somewhat close to the n=1 condition for elastic loading for which K is the relevant correlating parameter. It is possible that for materials with low n values, the difference between the stress fields under small and large creep conditions are not too significant such that K is adequate as the correlating parameter for crack growth rates.

CONCLUSIONS

1. Creep crack growth in the pyroceram glass-ceramic occurs both in a continuous and dis-continuous manner.

2. The damage processes associated with creep crack growth in the pyroceram include the nucleation, growth, and coalescence of grain boundary cavities into microcracks, as well as the propagation and linkage of microcracks with the main crack.

3. The microcrack density in the pyroceram glass-ceramic decreased with increasing distance from the crack tip in the same manner as the Riedel and Rice creep strain field.

4. Creep crack growth in the pyroceram obeys a critical accumulated effective creep strain criterion. Crack extension occurred when the accumulated effective creep strain near the crack tip reached approximately 2%. The critical strain criterion might, however. be a manifestation of a critical microcrack density or creep damage criterion.

5. A threshold exists in the creep crack growth curve of the pyroceram. The threshold appears to originate from the lack of damage accumulation in the near tip region when the K level is below a critical value.

ACKNOWLEDGEMENTS

REFERENCES

1. A. G. Evans and F. F. Lange, *Crack Propagation and Fracture in Silicon Carbide*, J. Mate. Sci., 10 [10] 1659-64 (1975).

2. F. F. Lange, *High-Temperature Strength Behavior of Hot-Pressed Si_3N_4: Evidence for Subcritical Crack Growth*, J. Am. Ceram. Soc., 57 [2] 84-87 (1974).

3. M. G. Mendiratta and J. J. Petrovic, *Slow Crack Growth from Controlled Surface Flaws in Hot-Pressed Si_3N_4*, J. Am. Ceram. Soc., 61 [5-6] 226-30 (1978).

4. K. D. McHenry and R. E. Tressler, *Fracture Toughness and High-Temperature Slow Crack Growth in SiC*, J. Am. Ceram. Soc., 63 [3-4] (1980).

5. E. J. Minford and R. E. Tressler, *Determination of Threshold Stress Intensity for Crack Growth at High Temperature in Silicon Carbide Ceramics*, J. Am. Ceram. Soc., 66 [5] 338-40 (1983).

6. H. G. Schmid, T. Haug, A. Bornhauser, V. Gerold, and R. F. Pabst, *Crack Growth in Al_2O_3 with 3 wt% Glassy Phase*, pp. 631-41 in **Deformation of Ceramics II**, Edited by R. E. Tressler and R. C. Bradt, Plenum Publishing Corporation, New York (1984).

7. N. J. Tighe, S. M. Wiederhorn, T. J. Chuang, and C. L. McDaniel, *Creep Cavitation and Crack Growth in Silicon Nitride*, pp. 587-604 in **Deformation of Ceramics II, Materials Science Research**, Vol. 18, Edited by R. E. Tressler and R. C. Brandt, Plenum Press, New York (1984)

8.   R. L. Tsai and R. Taj, *Creep Fracture in Ceramics Containing Small Amounts of a Liquid Phase*, Acta Metal., 30 1043-58 (1982)

9.   A. G. Evans and W. Blumenthal, *High-Temperature Failure in Ceramics*, pp. 423-48 in Fracture Mechanics of Ceramics, Vol. 6, Measurements, Transformations and High-Temperature Fracture, Edited by R. C. Bradt, A. G. Evans, D. P. H. Hasselman, and F. F. Lange, Plenum Press, New York (1985).

10.   W. Blumenthal and A. G. Evans, *High-Temperature Failure of Polycrystalline Aluminia: II. Creep Crack Growth and Blunting*, J. Am. Ceram. Soc., 67 [11] 751-59 (1984)

11.   K. Jakus, S. M. Wiederhorn, and B. J. Hockey, *Nucleation and Growth of Cracks in Vitreous-Bonded Aluminum Oxide at Elevated Temperatures*, J. Am. Ceram. Soc., 69 [10] 725-31 (1986)

12.   A. G. Evans and B. J. Dalgleish, *Some Aspects of the High Temperature Performance of Ceramics and Ceramic Composites*, Ceramic Engineering and Science Proceedings, 7 [9-10] 1073-1094 (1986).

13.   B. J. Dalgleish, E. Slamovich, and A. G. Evans, *High Temperature Failure of Ceramics*, J. Materials for Energy Systems, 8 [2] 211-225 (1986).

14.   R. A. Page, K. S. Chan, D. L. Davidson, and J. Lankford, *Micromechanics of Creep-Crack Growth in a Glass Ceramic*, J. Am. Ceram. Soc., 1990 (in press).

15. M. D. Thouless and A. G. Evans, *On Creep Rupture in Materials Containing an Amorphous Phase*, Acta Met., 34 [1] 23-31 (1986).

16. J. Lankford, *Strength of Monolithic and Fiber-Reinforced Glass Ceramics at High Rates of Loading and Elevated Temperature*, Ceram. Eng. Sci. Proc., 9 [7-8] 843-52 (1988).

17. J. Lankford, *Dynamic Compressive Fracture in Fiber-Reinforced Ceramic Matrix Composites*, Mater. Sci. & Eng., A107 261-68 (1989).

18. T. I. Barry, L. A. Lay, and R. Morrell, *High Temperature Mechanical Properties of Cordierite Refractory Glass Ceramics*, Proc. British Ceramic Soc., 24 67-84 (1975).

19. R. Raj and C. K. Chyung, *Solution-Precipitation Creep in Glass Ceramics*, Acta Met., 29 [1] 159-166 (1981).

20. R. F. Cooper, D. L. Kohlstedt, and K. Chyung, *Solution-Precipitation Enhanced Creep in Solid Liquid Aggregates Which Display a Non-Zero Dihedral Angle*, Acta Met., 37 [7] 1759-1771 (1989).

21. E. M. Heuse and G. *Partidge, Creep Testing of Glass-Ceramics*, J. Mat. Sci., 9 [8] 1255-1261 (1974).

22. A. Nagy, J. B. Campbell, and D. L. Davidson, *A High Temperature Cyclic Loading Stage for the SEM*, Review of Sci. Instruments, 55 [5] 778-782 (1984).
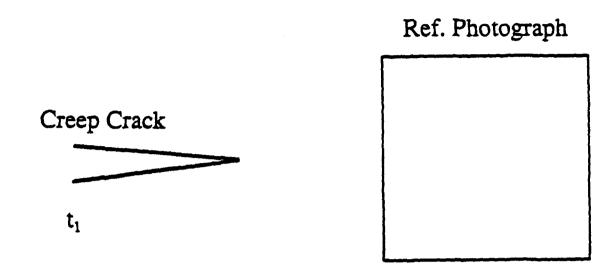
23. T. G. F. Gray, *Convenient Closed Form Stress Intensity Factors for Common Crack Configurations*, Int. J. Fract., 13 [1] 65-75 (1977).

24. E. A. Franke, D. J. Wenzel, and D. L. Davidson, *Measurement of Micro-Displacements by Machine Vision Photogrammetry (DISMAP)*, Rev. Sci. Inst. (in press).

25. D. R. Williams, D. L. Davidson, and J. Lankford, *Fatigue-Crack-Tip Plastic Strains by the Stereoimaging Technique*, Experimental Mech., 20 [4] 134-39 (1980).

26. B. Budiansky and R. J. O'Connell, *Elastic Moduli of a Cracked Solid*, Int. J. Solids Structures, 12 [2] 81-97 (1976).

27. E. E. Underwood, *The Mathematical Foundations of Quantitative Stereology*, pp. 3-38 in Stereology and Quantitative Metallography, ASTM STP 504, American Society for Testing and Materials, Philadelphia, PA (1972).

28. H. Riedel and J. R. Rice, *Tensile Cracks in Creeping Solids*, pp. 112-130 in Fracture Mechanics: Twelfth Conference, ASTM STP 700, American Society for Testing and Materials, Philadelphia, PA (1980).

29. H. Riedel and W. Wagner, *The Growth of Macroscopic Cracks in Creeping Materials*, pp. 683-690 in Advances in Fracture Research, Proceedings of the Fifth International Conferences on Fracture, Vol. 2, Edited by D. Francois, Pergamon, New York (1981).

30. H. Riedel, *Fracture at High Temperatures*, pp. 319-323, Springer-Verlug, Berlin, FR Germany (1986).

31.   M. D. Thoules and A. G. Evans, *Some Considerations Regarding the Creep Crack Growth Threshold*, **Scripta Met.**, 18 [10] 1175-1180 (1984).

LIST OF FIGURES

10. Traces of microcracks showing extensive microcracking in the pyroceram.

11. Maximum length of microcracks as function of distance, r, ahead of the tip of the main crack.

12. Number of microcracks as function of distance, r, ahead of the tip of the main crack.

13. Microcrack density parameter, ψ, as function of distance from the tip of the main crack.

14. TEM replica showing inhomogeneously distributed microcracks and grain boundary cavities associated with creep-crack growth in pyroceram.

15. Rows of equally spaced and sized cavities observed during creep-crack growth in pyroceram.

16. TEM replica showing a pocket of creep cavities surrounded by relatively uncavitated regions.

17. Heavily cavitated regions at both ends of a microcrack.

18. Comparison of the distributions of creep strain at K levels below and above the growth threshold, K_{th}. At $K > K_{th}$, creep-crack growth occurred by propagating along a localized shear zone formed ahead of the main crack. At $K < K_{th}$, a localized crack-tip shear zone was absent and no detectable crack growth was observed.
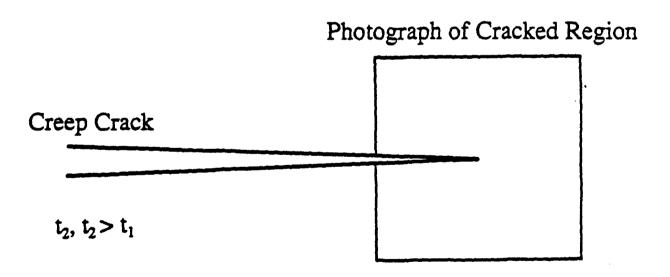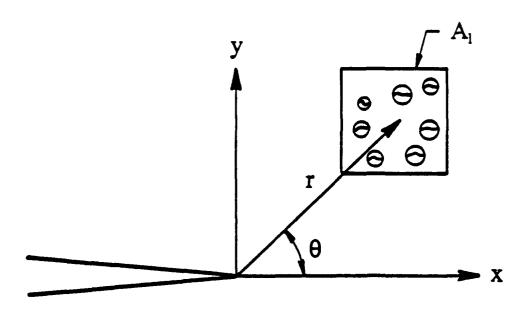
Figure 1.   Schematic showing the procedure for determining the accumulated creep strain using photographs of an area ahead of a creep crack in the uncracked and cracked conditions.

Legend:

ψ = Crack density parameter

n_i = No. of microcracks of length a_i

a_i = Half-length of a microcrack

A_l = Area within the sampling square

$$\psi = \frac{\pi}{A_l} n_i (a_i)^2$$

Figure 2.   Schematic showing the procedure for determining the microcrack density parameter, ψ, in a sampling area, A_l, located at a distance, r, and angle, θ, from the crack tip.
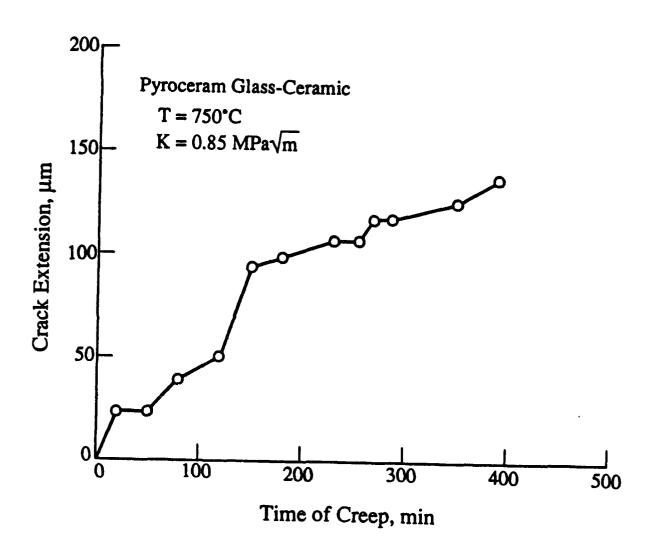
Figure 3.   Crack extension as a function of time of creep.

Main Crack

t_1

Microcrack t_2

t_3

t_4

t_5

t_1

t_2

t_3

t_4

Crack Extension

Crack
jump

t_4 t_5

No growth
period

t_2 t_3

t_1

No growth
period

Time of Creep

(a)

Crack Extension

t_4

t_3

t_2

t_1

Time of Creep

(b)
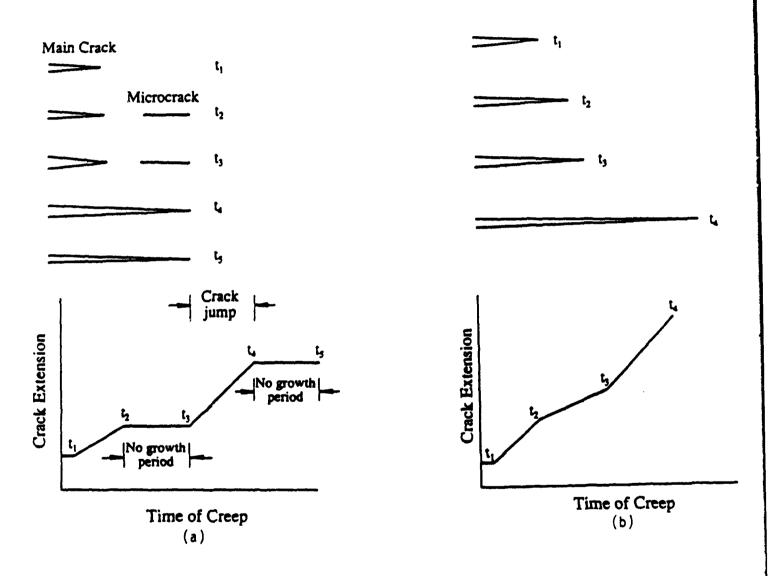
Figure 4. Schematic showing the creep-crack growth processes observed in the pyroceram glass-ceramic: (a) discontinuous crack growth, and (b) continuous crack growth.
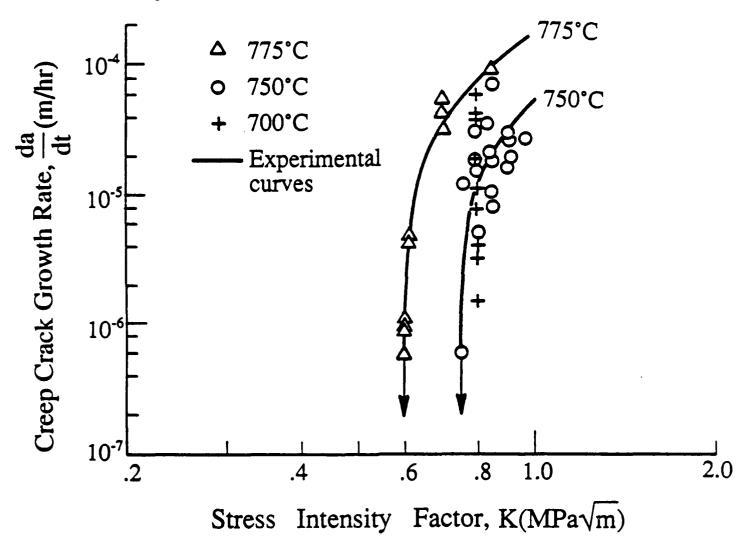
Figure 5. Creep-crack growth curves for the pyroceram glass-ceramic showing the existence of a growth threshold.
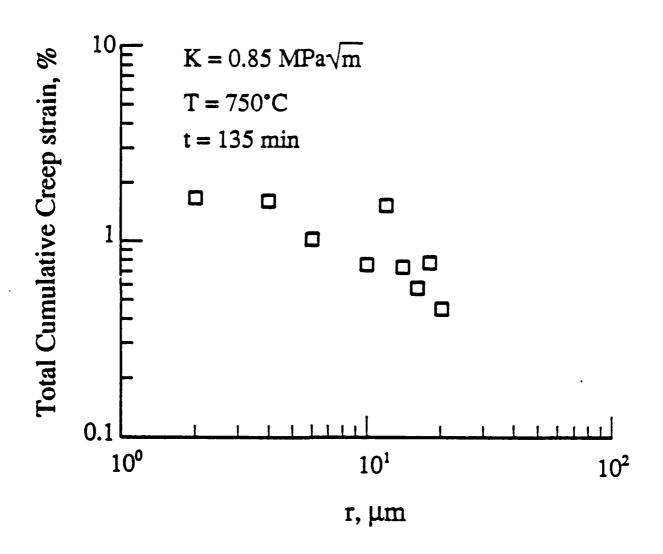
Figure 6.   Total cumulative creep strain as a function of distance, r, ahead of the crack tip showing the creep strain accumulated near the crack tip prior to crack growth is ≈ 2%.
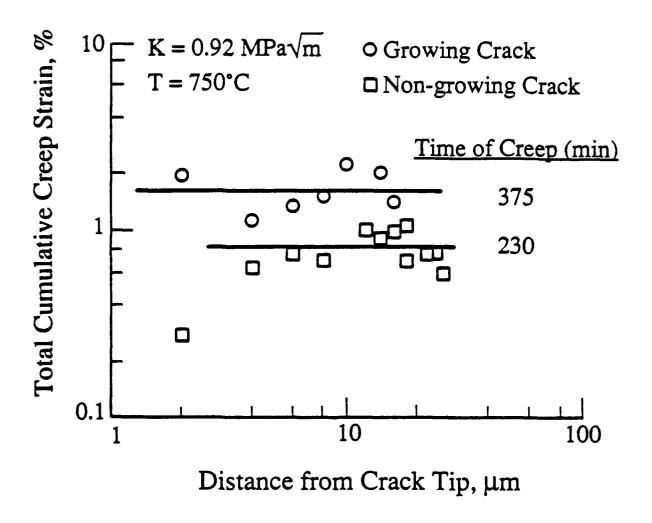
Figure 7. Comparison of total cumulative creep strains for a creep crack in the nonpropagating and propagating conditions.
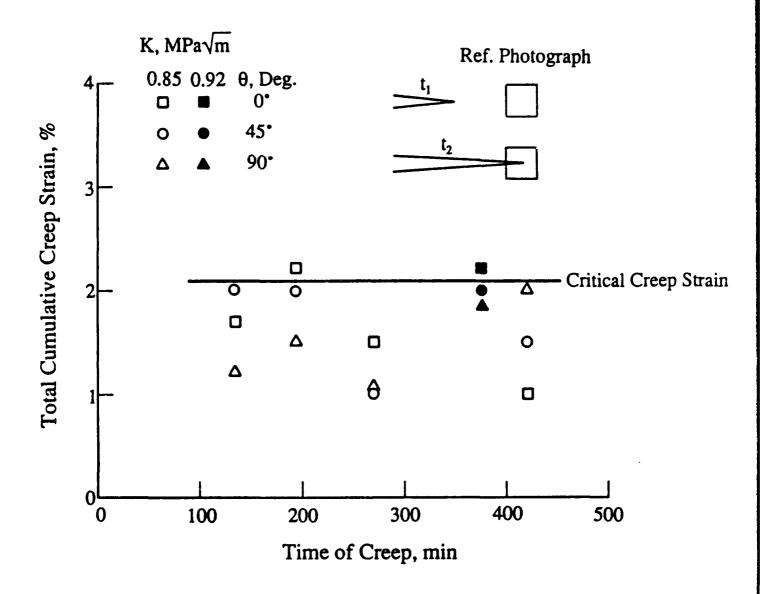
Figure 8.   Critical values of the total cumulative creep strain for various times of creep.

Figure 9.   Microcracks observed near the tip of the main crack in pyroceram.
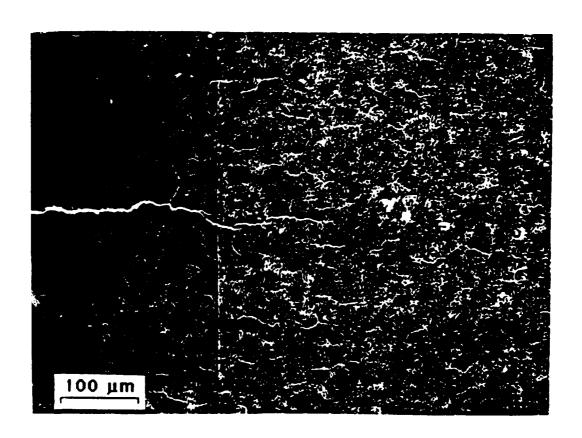
250 μm
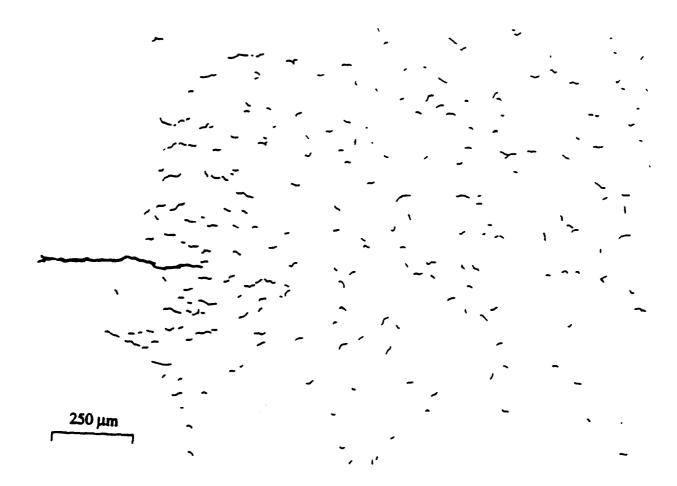
Figure 10.   Traces of microcracks showing extensive microcracking in the pyroceram.
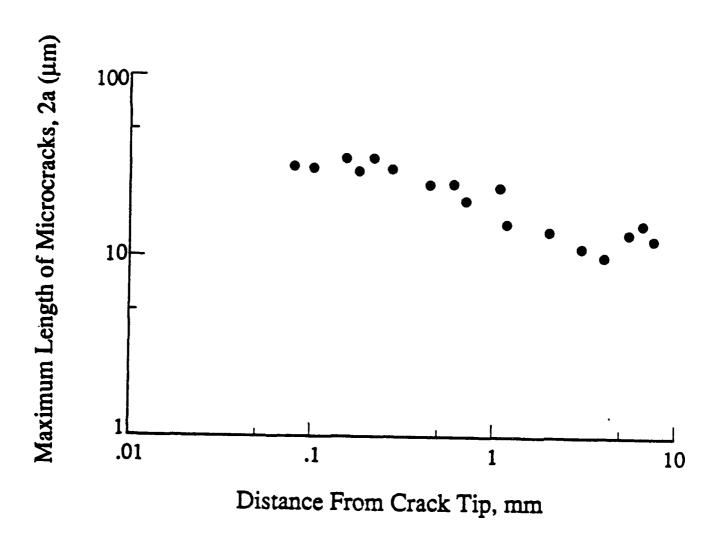
Figure 11.   Maximum length of microcracks as function of distance, r, ahead of the tip of the main crack.
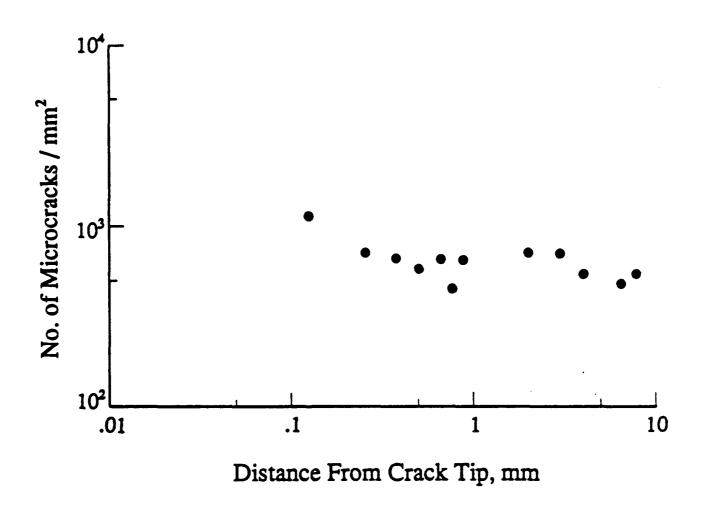
Figure 12.   Number of microcracks as function of distance, r, ahead of the tip of the main crack.
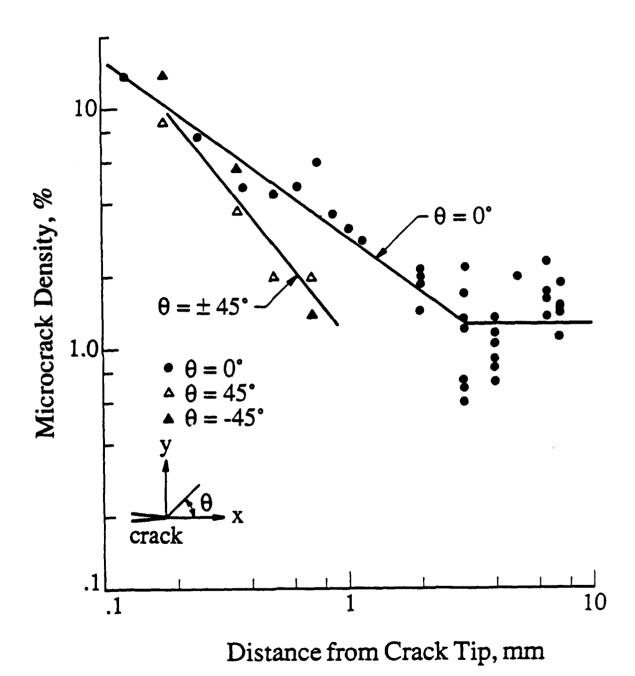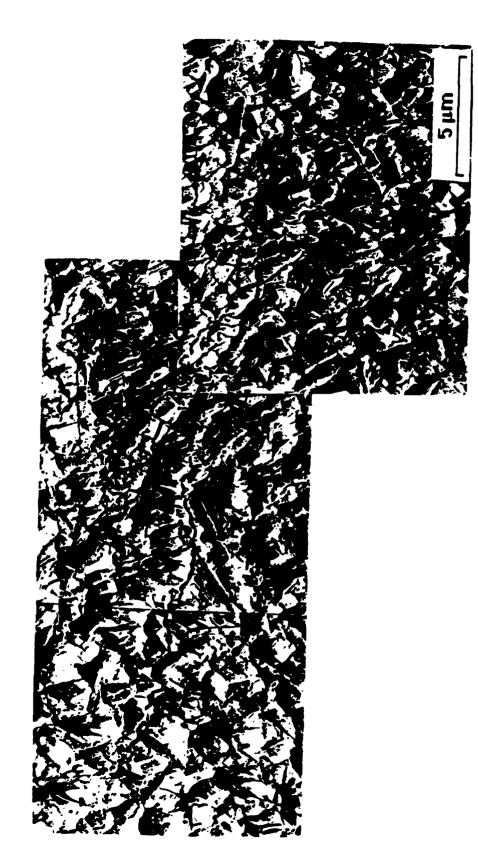
Figure 13. Microcrack density parameter, ψ, as function of distance from the tip of the main crack.

Figure 14. TEM replica showing inhomogeneously distributed microcracks and grain boundary cavities associated with creep-crack growth in pyroceram.
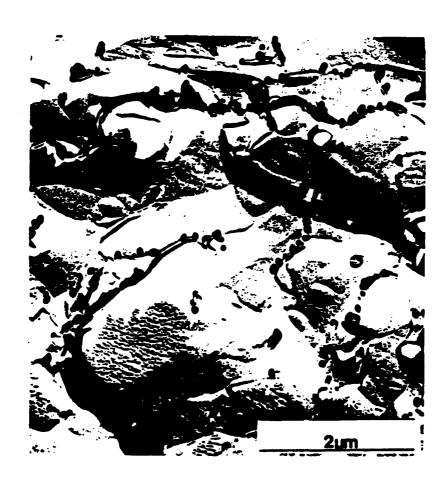
Figure 15. Rows of equally spaced and sized cavities observed during creep-crack growth in pyroceram.

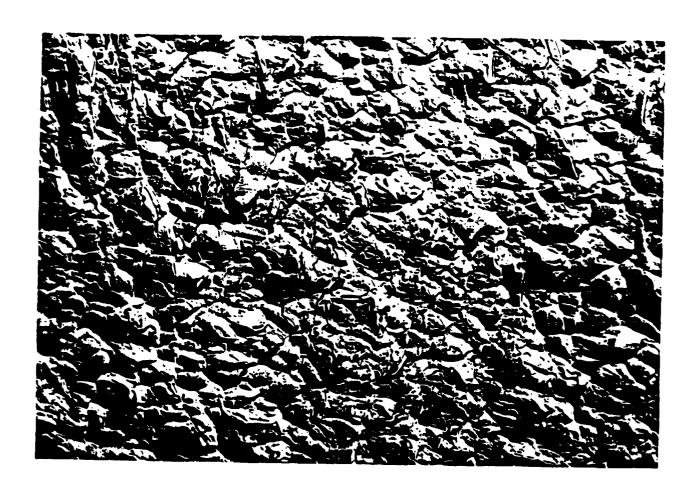Figure 16. TEM replica showing a pocket of creep cavities surrounded by relatively uncavitated regions.
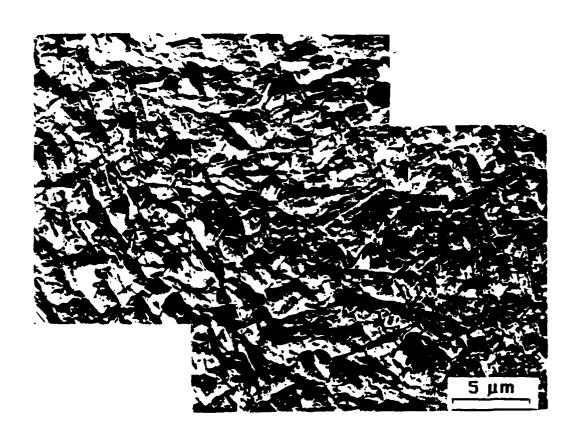
Figure 17. Heavily cavitated regions at both ends of a microcrack.
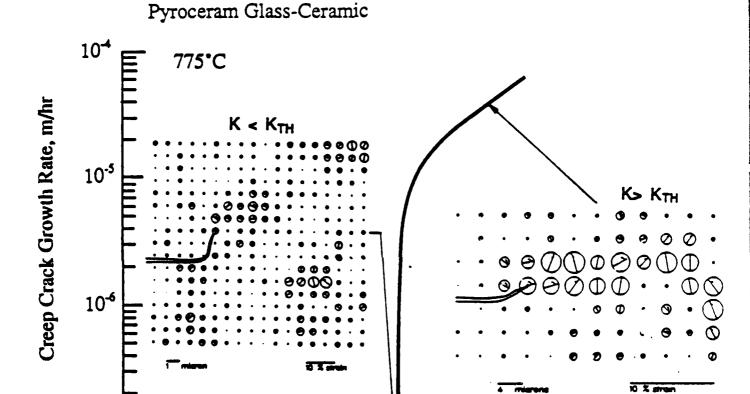
Pyroceram Glass-Ceramic

Figure 18.   Comparison of the distributions of creep strain at K levels below and above the growth threshold, K_{th}. At $K > K_{th}$, creep-crack growth occurred by propagating along a localized shear zone formed ahead of the main crack. At $K < K_{th}$, a localized crack-tip shear zone was absent and no detectable crack growth was observed.